# PIN OR NEEDLE FRAGMENT HR-3031 - TIN BRONZE - LATE BRONZE AGE - SWITZERLAND

| | |
|---|---|
| **Artefact name** | Pin or needle fragment HR-3031 |
| **Authors** | Marianne. Senn (EMPA, Dübendorf, Zurich, Switzerland) & Christian. Degrigny (HE-Arc CR, Neuchâtel, Neuchâtel, Switzerland) |
| **Url** | /artefacts/910/ |

## The object



*Credit HE-Arc CR.*

Fig. 1: Pin or needle fragment (after Rychner-Faraggi 1993, plate 74.11),

## Description and visual observation

| | |
|---|---|
| **Description of the artefact** | Pin or needle fragment (Fig. 1). The patina is green-blue and granulated, typical of terrestrial context. Dimensions: L = 9cm; Ø = 2.5-2.9mm; WT = 3.6g. |
| **Type of artefact** | Pin |
| **Origin** | Hauterive - Champréveyres, Neuchâtel, Neuchâtel, Switzerland |
| **Recovering date** | Excavation 1983-1985, object from layer 1 (containing material from the Bronze Age until the 20th century) |
| **Chronology category** | Late Bronze Age |
| **chronology tpq** | 1050 B.C. |
| **chronology taq** | 800 B.C. |
| **Chronology comment** | Hallstatt A2/B |
| **Burial conditions / environment** | Lake |
| **Artefact location** | Laténium, Neuchâtel, Neuchâtel |
| **Owner** | Laténium, Neuchâtel, Neuchâtel |


This work is licensed under CC BY-NC-ND 4.0

| | |
|---|---|
| **Inv. number** | Hr 3031 |
| **Recorded conservation data** | Not conserved |

**Complementary information**

Considered to be a land patina by Schweizer (1994).

## Study area(s)



*Credit HE-Arc CR.*

Fig. 2: Location of sampling area,

## Binocular observation and representation of the corrosion structure

None.

## MiCorr stratigraphy(ies) – Bi

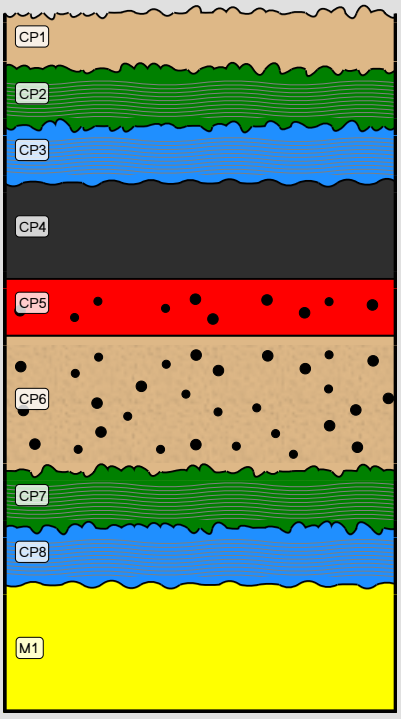
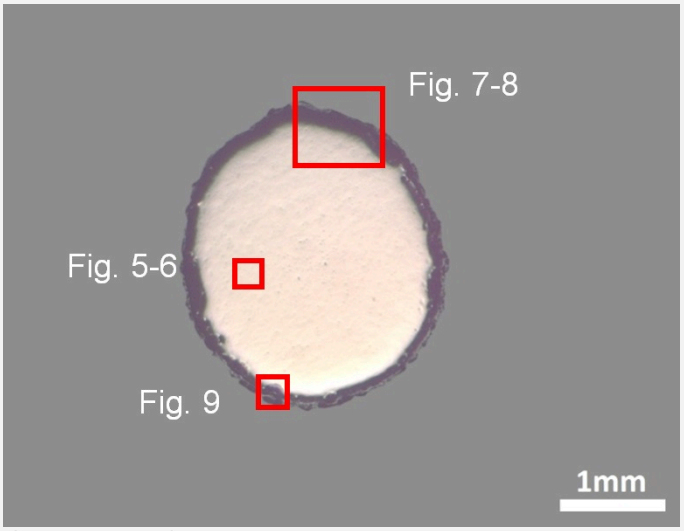



Fig. 3: Stratigraphic representation of the pin or needle fragment with green-blue patina under binocular using the MiCorr application. The characteristics of the strata are only accessible by clicking on the drawing that redirects you to the search tool by stratigraphy representation, Credit HE-Arc CR.


This work is licensed under CC BY-NC-ND 4.0

## Sample(s)




*Credit HE-Arc CR.*

Fig. 4: Micrograph of the cross-section of the sample taken from the pin or needle fragment with green-blue patina showing the location of Figs. 5 to 9,

| | |
|---|---|
| **Description of sample** | The cross-section is circular and is a complete section through the pin (Fig. 2). The surface is completely covered with a rather thin corrosion crust of irregular thickness (Fig. 4). |
| **Alloy** | Tin Bronze |
| **Technology** | Cold worked after annealing |
| **Lab number of sample** | MAH 87-195 |
| **Sample location** | Musées d'art et d'histoire, Genève, Geneva |
| **Responsible institution** | Musées d'art et d'histoire, Genève, Geneva |
| **Date and aim of sampling** | 1987, metallography and corrosion characterisation |

### Complementary information

This sample is mentioned in Schweizer, 1994.

## Analyses and results

***Analyses performed:***
Metallography (etched with ferric chloride reagent), Vickers hardness testing, ICP-OES, SEM/EDS, XRD.

## Non invasive analysis

None.


This work is licensed under CC BY-NC-ND 4.0

## Metal

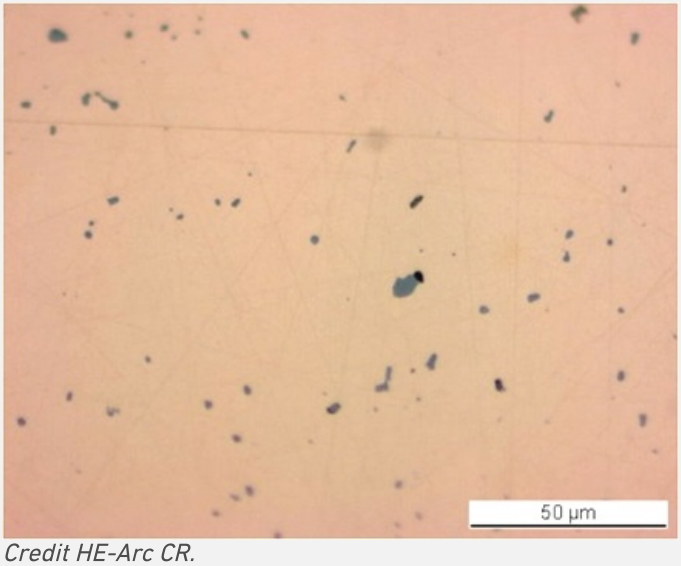
The remaining metal is a tin bronze and contains small copper sulphide and Pb-rich inclusions evenly distributed throughout the metal (Fig. 5, Tables 1 and 2). The Pb-rich inclusions are only visible with SEM appearing as white particles. The etched structure of the tin bronze shows re-crystallised and angular grains, some of them with twins (Fig. 6). Strain or slip lines are visible, especially near the metal surface. They indicate a final cold working. Copper sulphide inclusions are found both at the grain boundaries and inside the grains (Fig. 6). The average hardness of the metal is about HV1 120.

| Elements | Cu | Sn | Sb | Ni | As | Pb | Ag | Co | Zn | Fe |
|---|---|---|---|---|---|---|---|---|---|---|
| mass% | 91.29 | 5.65 | 1.00 | 0.69 | 0.55 | 0.51 | 0.22 | 0.06 | 0.01 | 0.02 |

Table 1: Chemical composition of the metal. Method of analysis: ICP-OES, Laboratory of Analytical Chemistry, Empa.

| Elements | S | Cu | Total |
|---|---|---|---|
| mass% | 21 | 85 | 106 |

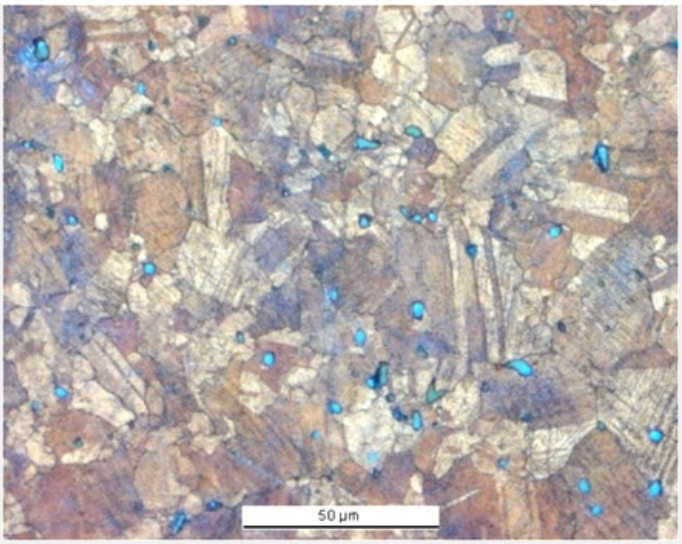
Table 2: Chemical composition of grey inclusions (Fig. 4). Method of analysis: SEM/EDS, Laboratory of Analytical Chemistry, Empa.




*Credit HE-Arc CR.*

Fig. 5: Micrograph of the metal sample from Fig. 4 (detail), unetched, bright field. Grey copper sulphide inclusions are clearly visible,


This work is licensed under CC BY-NC-ND 4.0




*Credit HE-Arc CR.*

Fig. 6: Micrograph of the metal sample from Fig. 4 (detail), etched, bright field. Small angular re-crystallised grains (some with twins) with slip lines are observed. Copper sulphide inclusions appear in blue,

| | |
|---|---|
| **Microstructure** | Polygonal and twinned grains + strain lines (metal surface) |
| **First metal element** | Cu |
| **Other metal elements** | Ni, As, Ag, Sn, Sb, Pb |

**Complementary information**

Schweizer (1994) indicates that the copper-tin alloys similar to the one of the pin have minor constituents that were certainly not added intentionally. Furthermore, he mentions that there is no systematic composition difference between bronzes with a lake patina and those with a land patina.

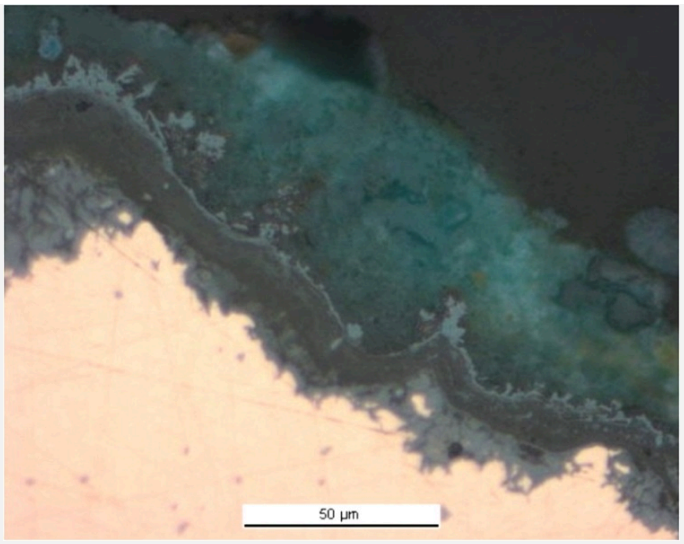
## Corrosion layers

The corrosion crust has an average thickness of about 50µm (Fig. 7). In polarised light (Fig. 8), the corrosion stratigraphy is more clearly visible: it is composed of an inner dark red-green-yellow corrosion layer (CP6 to CP8, an agglomerate of nanoscale stannic oxides with cuprite) directly on the metal core (Table 3 and Fig. 9, already studied by Piccardo et al. 2007), an intermediate multi-layered black-grey bands (CP3 to CP5) and an outer turquoise-green layer (CP1-CP2) analysed with XRD by Schweizer and identified as malachite/CuCO3Cu(OH)2 (Schweizer 1994). In some areas the dark-red layers (CP8) can also be found in between the black-grey bands (CP3 to CP5) and the malachite (CP1-CP2). Elemental chemical distribution of the SEM image of Fig. 9 shows that the black-grey layers are enriched in Sn but also contain Fe. Superior markers such as contextual Al and Si are present in the outer malachite layers. S is present both on the rim of the outer black-grey layers and in the malachite (Fig. 9, Table 3).

| Elements | O | Cu | Sn | S | Cl | Fe | As | Ag | Total |
|---|---|---|---|---|---|---|---|---|---|
| CP6 | 20 | 40 | 12 | 15 | < | 5 | < | 1.9 | 94 |
| CP8 | 20 | 53 | 16 | < | 0.9 | < | 0.6 | < | 91 |

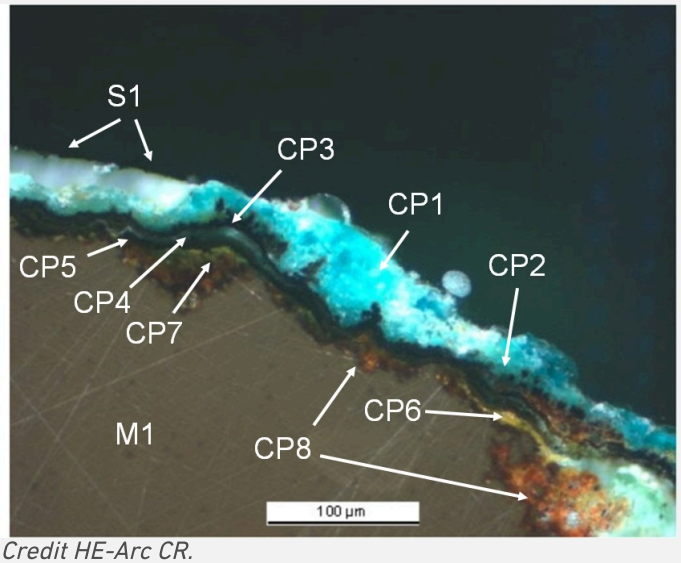
Table 3: Chemical composition (mass %) of orange corrosion products (from Figs. 8 and 9). Method of analysis: SEM/EDS, Laboratory of Analytical Chemistry, Empa.


This work is licensed under CC BY-NC-ND 4.0



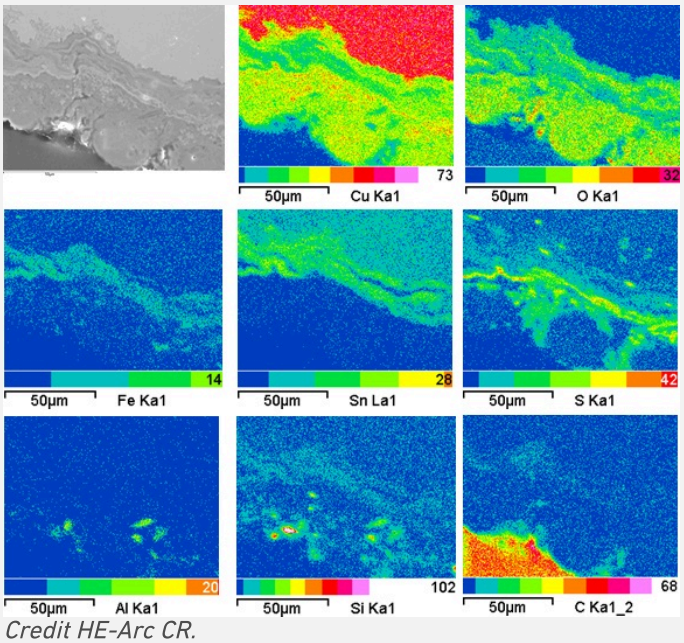

*Credit HE-Arc CR.*

Fig. 7: Micrograph of the metal sample from Fig. 4 (detail) and corresponding to the stratigraphy of Fig. 10, unetched, bright field. Stratigraphy of the corrosion crust: inner light grey layer (CP3), intermediate dark grey layer with a light-grey rim (CP2) and outer grey-green layer (CP1),




*Credit HE-Arc CR.*

Fig. 8: Micrograph of the metal sample from Fig. 4 and corresponding to the stratigraphy of Fig. 10, polarised light. The metal appears in brown; the inner layer appears as red-orange, the intermediate layer as black and the outer layer as turquoise,




*Credit HE-Arc CR.*

Fig. 9: SEM image, SE-mode, and elemental chemical distribution of a selected area of Fig. 4. Method of examination: SEM/EDS, Laboratory of Analytical Chemistry, Empa,

**Corrosion form** Multiform - pitting


This work is licensed under CC BY-NC-ND 4.0

**Corrosion type** Type II (Robbiola)

### Complementary information

None.

## MiCorr stratigraphy(ies) – CS

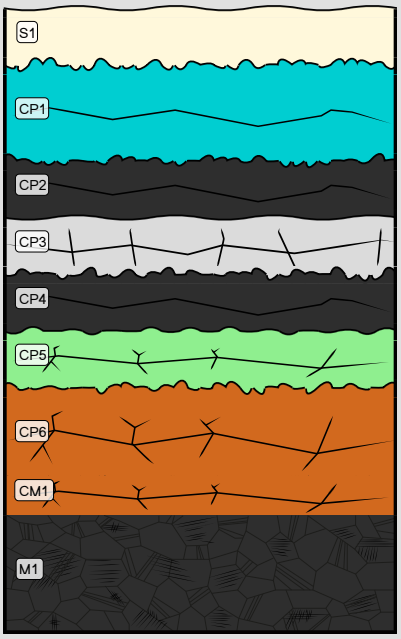



Fig. 10: Stratigraphic representation of the sample taken from the pin or needle fragment with green-blue patina in cross-section (dark field) using the MiCorr application. The characteristics of the strata are only accessible by clicking on the drawing that redirects you to the search tool by stratigraphy representation. This representation can be compared to Figs. 7 and 8, Credit HE-Arc CR.

## Synthesis of the binocular / cross-section examination of the corrosion structure

The two corrosion structures observed under binocular and on cross-sections look rather different. It might be due to some disruption during the cutting process.

## Conclusion

The pin is made from a tin bronze and has been repeatedly cold worked and annealed. After the last annealing there has been some cold work, as can be seen from the strain lines visible after etching the metal. Due to the presence in the corrosion crust of an outer malachite layer, the corrosion was described as terrestrial by Schweizer (Schweizer 1994). The elemental chemical distribution of the corrosion crust shows a more complex situation: as expected for an object buried in a terrestrial site, a typical enrichment of Sn is observed in the inner and intermediate layers covering the remaining metal surface. However it is combined with Fe and S which are often present in lake patinas. According to Schweizer, these layers were formed in anaerobic conditions and developed later on into malachite in an aerated soil through partial dehydration (Schweizer 1994, Schwartz 1934). Since the original surface is absent (destroyed), we refer to type 2 corrosion after Robbiola et al. 1998.


This work is licensed under CC BY-NC-ND 4.0

## References

### References on object and sample


*References object*

1. Rychner-Faraggi A-M. (1993) Hauterive – Champréveyres 9. Métal et parure au Bronze final. Archéologie neuchâteloise, 17 (Neuchâtel), planche 74.11.

*References sample*

2. Empa Report 137 695/1991, P.O. Boll.
3. Rapport d'examen, Laboratoire Musées d'art et d'Histoire, Geneva GE (1987), 87-194 à 197.
4. Schwartz, G.M. (1934) Paragenesis of oxidised ores of copper, Economic Geology, 29, 55-75.
5. Schweizer, F. (1994) Bronze objects from Lake sites: from patina to bibliography. In: Ancient and historic metals, conservation and scientific resarch (eds. Scott, D.A., Podany, J. and Considine B.B.), The Getty Conservation Institute, 33-50.


### References on analytic methods and interpretation


6. Interpretation of orange corrosion products, see: Piccardo P., Mille B., Robbiola L. (2007) Tin and copper oxide in corroded archaeological bronzes, In: Corrosion of metallic heritage artefacts, European Federation of Corrosion Publication n°48, ed. Dillmann et al., 239-262.
7. Robbiola, L., Blengino, J-M., Fiaud, C. (1998) Morphology and mechanisms of formation of natural patinas on archaeological Cu-Sn alloys, Corrosion Science, 40, 12, 2083-2111.



This work is licensed under CC BY-NC-ND 4.0